Anti-inflammatory effect of trans-4-methoxycinnamaldehyde from *Etlingera pavieana* in LPS-stimulated macrophages mediated through inactivation of NF-κB and JNK/c-Jun signaling pathways and in rat models of acute inflammation

Klaokwan Srisook[a,b,*], Sakulrat Mankhong[a,b], Natthakarn Chiranthanut[c], Kittiya Kongsamak[a], Na-thanit Kitwiwat[a], Patsara Tongjurai[a], Pornpun Aramsangtienchai[a]

[a] *Department of Biochemistry, Faculty of Science, Burapha University, Chonburi 20131, Thailand*
[b] *Center of Excellence for Innovation in Chemistry, Burapha University, 20131, Thailand*
[c] *Department of Pharmacology, Center of Excellence for Innovation in Chemistry, Faculty of Medicine, Chiang Mai University, Chiang Mai 50200, Thailand*

ARTICLE INFO	ABSTRACT
	Trans-4-methoxycinnamaldehyde (MCD) was isolated from the rhizomes of *Etlingera pavieana* (Pierre ex Gagnep.) R.M.Sm. MCD shows anti-inflammatory effects. However, the molecular mechanism underlying its anti-inflammatory action has not been described. In this study, we investigated this mechanism in lipopolysaccharide (LPS)-induced RAW 264.7 macrophages and found MCD significantly inhibited nitric oxide (NO) and prostaglandin E$_2$ (PGE$_2$) production in a concentration-dependent manner. MCD could decrease LPS- and Pam3CSK4- induced the expressions of both iNOS and COX-2. The phosphorylation of inhibitory κB (IκB) and translocation of nuclear factor-κB (NF-κB) p65 subunit into the nucleus were also inhibited by MCD. Moreover, MCD suppressed LPS-induced phosphorylation of JNK except for ERK and p38 mitogen-activated protein kinases (MAPKs). Moreover, MCD significantly reduced ethyl phenylpropiolate-induced ear edema and carrageenan-induced paw edema in rat models. These findings indicated MCD has anti-inflammatory activity by inhibiting the production of NO and PGE$_2$ by blocking NF-κB and JNK/c-Jun signaling pathways. Collectively, these data suggest that MCD could be developed as a novel therapeutic agent for inflammatory disorders.

1. Introduction

Inflammation is an innate immune process that rids the body of invading pathogens or irritants (Abbas and Lichtman, 2003). In the course of activation by pathogens, macrophages secrete a series of inflammatory mediators such as nitric oxide (NO), prostaglandins (PGs) and inflammatory cytokines such as tumor necrosis factor-α (TNF-α) and interleukin-1 β (IL-1β) (Fujiwara and Kobayashi, 2005; Christiansen, Nielsen, and Kolte, 2006). Overproduction and prolonged secretion of these mediators and cytokines are involved in a variety of acute and chronic inflammation-related diseases (Qureshi et al., 2011) with their inhibition being a major target of anti-inflammatory agents.

Lipopolysaccharide (LPS), a main component of Gram-negative bacteria, activates toll-like receptor (TLR)-4 that regulate immune responses in macrophages via downstream signaling cascades, including nuclear factor-κB (NF-κB)/inhibitory κB (IκB) and mitogen activated protein kinase (MAPK) pathways (Lu, Yeh, and Ohashi, 2008; Achek, Yesudhas, and Choi, 2016). The classical MAPKs are ERK, JNK and p38 MAPK (Udomphong, Mankhong, Jaratjaroonphong, and Srisook, 2017). Activation of NF-κB/IκB and MAPKs pass on the signal for inducing transcription activity of NF-κB and activator protein-1 (AP-1), which regulate the transcription of various inflammation-related genes, such as inducible nitric oxide synthase (iNOS), cyclooxygenase-2 (COX-2) and inflammatory cytokines, (Prekumar, Dey, Dorn, and Raskin, 2010, Baker, Hayden, and Ghosh, 2011, Santos et al., 2011).

Rhizome of *Etlingera pavieana* (Pierre ex Gagnep.) R.M.Sm. (Family Zingiberaceae) is used as a spice and a traditional medicine in Thailand and Cambodia (Tachai and Nuntawong, 2016; Poulsen and Phonsena, 2017). *Trans*-4-methoxycinnamaldehyde (MCD) (Fig. 1) is one of the phenolic compounds isolated from the rhizomes of this plant (Tachai and Nuntawong, 2016; Srisook, Palachot, Mankhong, and Srisook, 2017). MCD has been reported to exert anti-viral, anti-bacterial and

---
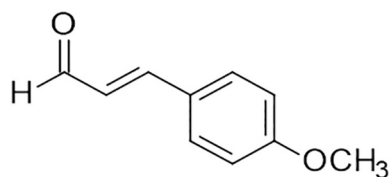
Fig. 1. Chemical structure of trans-4-methoxycinnamaldehyde (MCD).

anti-tumor activities (Wang, Chang, Chiang, and Lin, 2009; Sharma et al., 2013; Iawsipo, Srisook, Ponglikitmongkol, Tatiyar, and Singaed, 2018); recently, it has also been reported to inhibit inflammation by suppressing NO production in LPS-induced RAW 264.7 macrophages (Srisook, Palachot, Mankhong, and Srisook, 2017). However, the mechanistic understanding of its actions has not been explored. The objective of this study was to determine the mechanisms associated with this anti-inflammatory effect in a macrophage cell model. Furthermore, the anti-inflammatory activity of MCD on acute inflammation of ear and paw edema in rats was investigated.

2. Materials and methods

2.1. Materials and chemicals

Trans-4-methoxycinnamaldehyde (MCD) was isolated from *E. pavieana* rhizomes as described by Srisook et al. (Srisook, Palachot, Mankhong, and Srisook, 2017) and kindly provided by Dr. E. Srisook, Department of Chemistry, Burapha University. A nucleospin RNA kit was purchased from Macherey-Nagel (Düren, Germany). A $5\times$ iScript™ Reverse Transcription Supermix for RT-qPCR, $2\times$ iTaq™ Universal SYBR Green supermix), and Quick Start Bradford protein assay kit were obtained from Bio-Rad (Hercules, CA, USA). Antibodies for GAPDH, NF-κB p65, phospho-IκB-α (Ser32/36), phospho-SAPK/JNK (Thr183/Tyr185), phospho-p38 MAPK (Thr180/Tyr182), phospho-ERK1/2 (Thr202/Tyr204), phospho-c-Jun (Ser63), phospho-STAT-1 (Ser727) and total SAPK/JNK, anti-mouse and–rabbit IgG, HRP-linked antibody, anti-Rabbit IgG (H + L), F(ab')2 Fragment (Alexa fluor® 488 conjugate) were obtained from Cell Signaling Technology (Beverly, MA, USA). Antibodies for iNOS and COX-2 were obtained from BD Bioscience (San Jose, CA, USA). A Prostaglandins E2 Enzyme Immunoassay Kit was obtained from Arbor Assays (Ann Arbor, MI, USA.). Lipopolysaccharide or LPS (*Escherichia coli* serotype O111:B4) and 3-(4,5-dimethylthiazol-2-yl)-2,5-diphenyltetrazolium bromide (MTT) were purchased from Sigma Chemical (St. Louis, MO, USA). Invitrogen prolong gold antifade reagent with DAPI was purchased from Thermo Fisher Scientific (Waltham, MA, USA). Antibodies for total ERK1/2 and total p38 MAPK were obtained from Santa Cruz Biotechnology (Dallas, TX, USA). Synthetic triacylated lipoprotein (Pam3CSK4) was purchased from InvivoGen (San Diego, CA, USA).

2.2. Cell culture and sample treatment

Macrophage cell line RAW 264.7 was obtained from ATCC (Rockville, MD, USA). Cells were suspended in Dulbecco's Modified Eagle Medium (DMEM) containing 100 U/mL of penicillin, 100 μg/mL of streptomycin and 10% heat-inactivated FBS and were cultured at 37 °C in humidified air containing 5% CO_2. MCD was dissolved in dimethyl sulfoxide (DMSO), and subsequently passed through a 0.22-μm sterile filter. Cells were treated with MCD at indicated concentrations and 1 μg/mL LPS for 24 h.

2.3. Cell viability assay

Cell viability was determined by a 3-(4,5-dimethylthiazol-2-yl)-2,5-diphenyltetrazolium bromide (MTT) assay. The formation of MTT-formazan is proportional to the number of cells that are still alive. The

method was carried out as reported by Srisook et al. (Srisook, Palachot, Mongkol, Srisook, and Sarapusit, 2011).

2.4. Nitrite assay and determination of PGE_2

Nitrite amounts present in the culture supernatant were used as an indicator of NO production. Its concentration was measured with a spectrophotometric assay based on the Griess reaction (Srisook et al., 2011). Production of PGE_2 in the conditioned media was determined using EIA kits according to the manufacturer's instructions. Production percentages were calculated as follows: (concentration of target molecule in medium from MCD-treated cells/ concentration of target molecule in medium from LPS-induced cells) × 100 and % inhibition of target molecule = 100 - % production of target molecule.

2.5. Western blot analysis

Macrophages (1×10^6 cells) were plated on 60-mm tissue culture plates and treated with different concentrations of MCD and LPS, and then were scraped in the presence of ice-cold RIPA lysis buffer containing a mixture of protease inhibitors and phosphatase inhibitors. The cell lysates were centrifuged at $13,700g$ for 10 min at 4 °C. Equal amounts of the supernatant proteins were separated by 10% SDS-polyacrylamide gel electrophoresis. Separated proteins were transferred onto PVDF membranes and nonspecific bindings were blocked with TBS-T buffer containing 5% (*w/v*) skim milk for 1 h at room temperature. The membrane was then incubated further with primary antibodies against iNOS, COX-2, GAPDH, p-IκB, p-cJun and MAPKs (1:1000 dilution). After washing with TBS-T buffer, the membrane was incubated with goat anti-rabbit or goat anti-mouse IgG conjugated to HRP secondary antibodies (1:5000 dilution). The specific protein bands on the PVDF membrane were visualized on X-ray film activated by ECL using the SuperSignal West Pico Chemiluminescent substrate.

2.6. Real-time reverse transcription-polymerase chain reaction (real-time RT-PCR)

Cells were stimulated with LPS and MCD for 9 h. Total cellular RNA was isolated using a Nucleospin RNA kit according to manufacturer's instructions. From each sample, 2 μg of total RNA were reverse-transcribed to make cDNA using $5\times$ iScript™ Reverse Transcription Supermix for RT-qPCR. The reaction mixture was incubated at 25 °C for 5 min, 42 °C for 30 min, and then at 85 °C for 5 min. Real-time RT-PCR was conducted on a CFX96 Touch Real time PCR (Bio-Rad, USA.) The reaction mixture for real-time PCR contained $2\times$ iTaq™ Universal SYBR Green supermix, cDNA and a specific primer. The primer for iNOS were 5′-GCACAGCACAGGAAATGTTTCAGCAC-3′ (F) and 5′ –AGC CAGCGT ACCGGATGAGC- 3′ (R); for COX-2 were 5′-TGATCGAAGACTACGTG CAA CACC-3′ (F) and 5′-TTCAATGTTGAAGGTGTCGGGCAG- 3′ (R); for EF-2 were 5′-CTGA AGCGGCTGGCTAAGTCTGA-3′ (F) and 5′-GGGTC AGATTTCTTGATGGGGTG-3′ (R), as described by Udompong et al. (Udomphong, Mankhong, Jaratjaroonphong, and Srisook, 2017). Amplification conditions were used as follows: 95 °C for 3 min for 1 cycle, then 95 °C for 10 s and 63 °C for 20 s for 40 cycles. Relative gene expression was calculated using $2^{-\Delta\Delta ct}$ to compare the mRNA level between the control and the treated cells (Giulietti et al., 2001).

2.7. Immunofluorescence and confocal microscopy

The effect of MCD on translocation of NF-κB p65 was investigated using immunofluorescence and a confocal microscopy technique with slight modifications from Udompong et al. (Udomphong, Mankhong, Jaratjaroonphong, and Srisook, 2017). Briefly, cells were seeded onto glass coverslips in a 6-well culture plate. After cell attachment, cells were pretreated with 37.5 μM MCD for 1 h and subsequently incubated with LPS (1 μg/mL) for 30 min. Cells were washed twice with PBS and

fixed with 4% (w/v) paraformaldehyde solution for 30 min at room temperature. Subsequently, the cells were permeabilized with 0.2% (v/v) Triton-X100 for 10 min at room temperature and blocked with 0.5% (w/v) BSA dissolved in PBS at room temperature for 1 h. Then, cells were incubated with anti-NF-kB p65 dissolved in 1% (w/v) BSA solution overnight at 4 °C. Then, cells were rinsed three times with PBS, each for 5 min, before incubation with anti-rabbit IgG (H + L) F(ab') fragment AlexaFluor 488 conjugate (1:500 dilutions) dissolved in 1% (w/v) BSA solution at room temperature for 1 h. Cells were counterstained and mounted with prolong gold antifade reagent with DAPI for 24 h. NF-kB p65 localization was visualized with an FV1000 Olympus confocal laser scanning microscope with excitation laser beams of 488 and 358 nm. Cell images were captured using ×60 objective oil-immersion lenses with ×2 zoom 640 × 640 pixel resolution.

2.8. Anti-inflammatory study in rat models

2.8.1. Experimental animals

Male Sprague–Dawley (SD) rats (40–60 g and 100–120 g) were purchased from the National Laboratory Animal Centre, Mahidol University, Nakhorn Pathom, Thailand. The rats were then maintained at the facility of medicine, Chiang Mai University. The animals were housed in groups of five rats per cage in standard metal cages in an animal room maintained at 24 ± 1 °C with relative humidity 50 ± 10% and a 12 h light - 12 h dark cycle throughout the study. All rats had access to food and water ad libitum. All experiments were approved by the Animal Ethics Committee, Burapha University (No: IACUC 014/2561) and Chiang Mai University (No: 20/2561).

2.8.2. Ethyl phenylpropiolate (EPP)-induced ear edema in rats

The experiment was carried out as described previously by Brattsand et al. (Brattsand, Thalen, Roempke, Kallstrom, and Gruvstad, 1982). Male rats (40–60 g) were used and divided into 3 groups of 3 rats (6 ears): control, reference and test groups. Ear edema was induced by topical application of EPP at a dose of 1 mg/20 μL/ear to the outer and inner surfaces of both ears of each rat. Immediately after the application of EPP, acetone (20 μL/ear), phenylbutazone (1 mg/20 μL/ear) or MCD extract (3 mg/20 μL/ear) was applied to the ears. Ear thickness was measured by digital Vernier calipers before and at 15, 30, 60 and 120 min after EPP application.

2.8.3. Carrageenan-induced hind paw edema in rats

The experiment was carried out according to the method of Winter et al. (Winter, Risley, and Nuss, 1962). Male rats (100–120 g) were used and divided into 5 groups of 6 rats: control, reference and 3 test groups. Paw edema was induced by injecting 0.05 mL of 2% carrageenan (in NSS) into the subplantar tissues of the left hind paw of each rat. The vehicle (5% Tween 80), aspirin (300 mg/kg) or MCD (75, 100 and 300 mg/kg) was given to each rat by oral gavage at 1 h before carrageenan injection. Swelling of carrageenan-injected feet was measured at 0, 1, 3 and 5 h with a plethysmometer (Ugo Basile). The degree of edema formation was determined as an increase in paw volume.

2.9. Statistical analysis

Results are expressed as the mean ± S.D. of at least three independent experiments. Statistical significance was tested using analysis of variance (ANOVA), followed by Tukey's test for multiple comparisons. A value of $P < .05$ was considered significant.

3. Results

3.1. Effect of MCD on cell viability of RAW 264.7 macrophages

Cytotoxicity of MCD against RAW 264.7 macrophages was determined using an MTT assay. MCD did not affect cell viability at
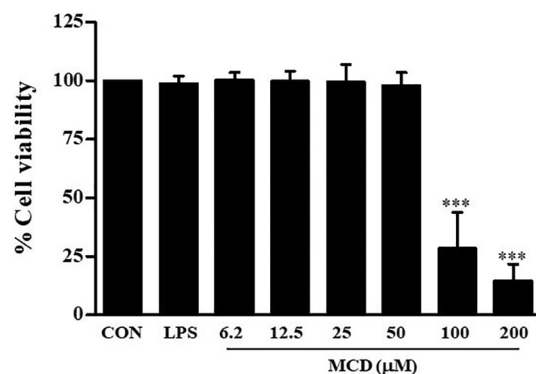
Fig. 2. MCD effect on cell viability. Cells were incubated with MCD at 6.2–200 μM for 24 h. Viability of cells was determined using MTT test. Each column shows the mean ± SD of three independent experiments with triplicate samples. ***$p < .001$ vs. control cells. CON = unstimulated control cells, LPS = LPS-stimulated cells.

concentrations of 6.2–50 μM (Fig. 2). However, cell viability after MCD treatment at 100–200 μM was markedly reduced. Subsequent treatment with MCD was restricted to 50 μM to exclude an MCD cytotoxic effect against RAW 264.7 macrophages.

3.2. Inhibitory effect of MCD on the LPS-stimulated NO and PGE$_2$ production

We determined the MCD effect on the formation of iNOS-catalyzed NO and COX-2-catalyzed PGE$_2$ on LPS-induced RAW 264.7 cells. LPS significantly increased the amount of NO and PGE$_2$ in RAW 264.7 cells compared to unstimulated control cells, while MCD significantly inhibited LPS-induced NO and PGE$_2$ production in a concentration-dependent manner (Fig. 3A and B).

3.3. MCD inhibited the expression of iNOS and COX-2 in macrophages

We next determined whether the decrease in NO and PGE$_2$ production is correlated with protein and mRNA expression of iNOS and COX-2 expression, respectively. In unstimulated cells, iNOS and COX-2 proteins were below the level of detection. In contrast, iNOS and COX-2 protein levels increased prominently in the presence of LPS (Fig. 3C-and 3D). MCD treatment suppressed LPS-activated protein levels of iNOS and COX-2 in a concentration-dependent manner. Similarly, MCD was found to suppress the levels of iNOS and COX-2 mRNA as determined by real-time RT-PCR (Fig. 3E and F).

The effect of MCD on Pam3CSK4-induced iNOS and COX-2 expression was also examined. We found that Pam3CSK4, an agonist of TLR2/1, significantly enhanced the protein levels of iNOS and COX-2. However, the expression was concentration-dependently suppressed by MCD in RAW 264.7 macrophages, as shown in Fig. 4A and B.

3.4. Inhibitory effect of MCD on LPS-induced NF-κB activation in macrophages

We then examined whether NF-κB activation is involved with the inhibitory effect of MCD on iNOS and COX-2 expressions. As determined by Western blot analysis, p-IκB increased in cells treated with LPS compared to control unstimulated cells (Fig. 5A). MCD at 50 μM slightly but significantly suppressed the phosphorylation of IκB at Ser32/36. Moreover, LPS induced nuclear translocation of NF-κB p65 as determined by immunofluorescence. However, MCD notably prevented LPS-induced NF-κB p65 nuclear translocation (Fig. 5B).
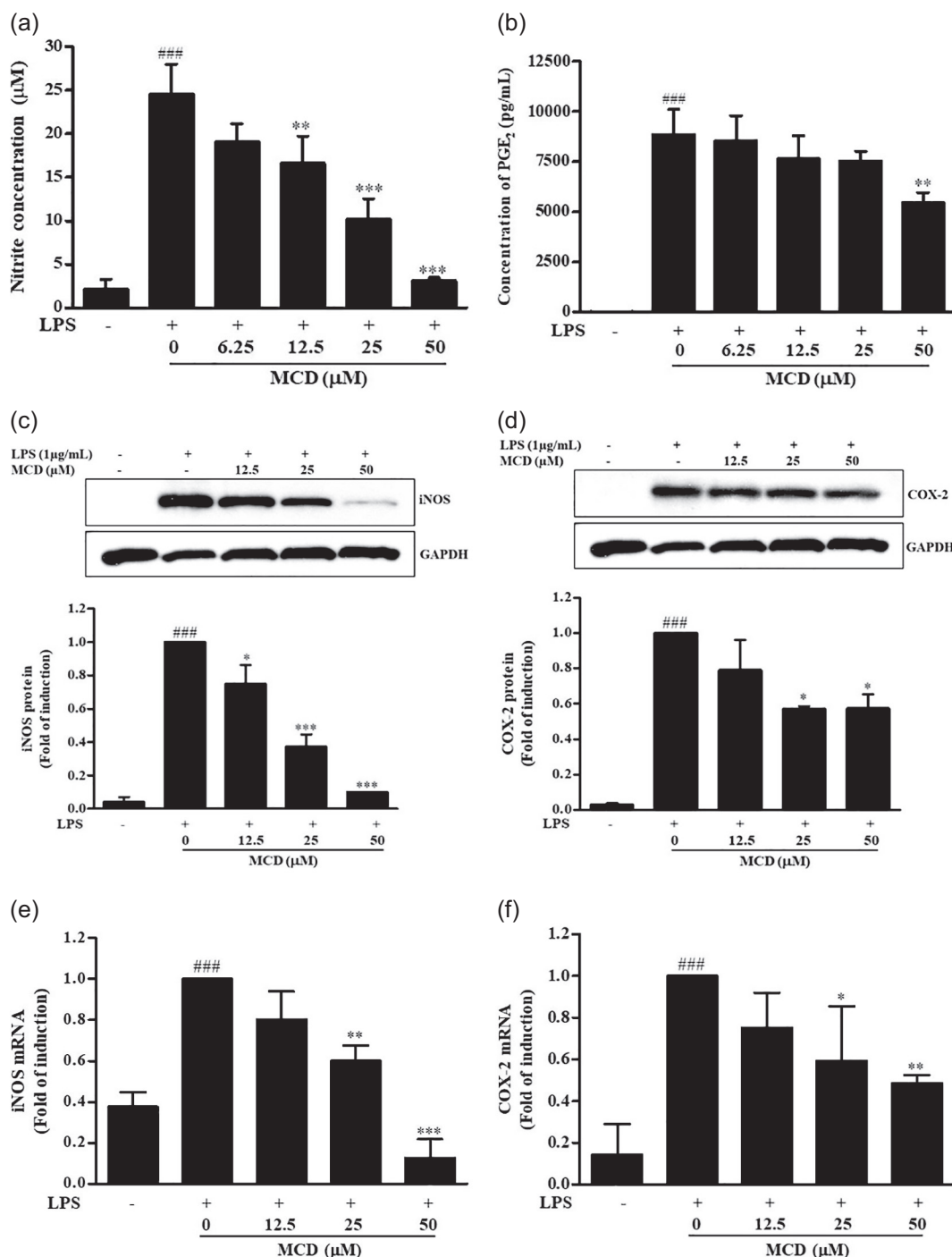
Fig. 3. Effect of MCD on NO and PGE$_2$ production as well as iNOS and COX-2 expression in LPS-stimulated RAW 264.7 macrophages. Cells were treated with MCD in the presence of 1 μg/mL LPS for 24 h. Concentrations of nitrite (A) and PGE$_2$ (B) in conditioned media are shown. The protein and mRNA levels of iNOS and COX-2 were determined by Western blot analysis (C, D) and real-time RT-PCR (E, F), respectively. The graph presents the mean ± SD ($n=3$) of densitometric values of iNOS or COX-2 proteins normalized with GAPDH. Data are expressed as folds of induction of LPS treated cells. $^{###}p < .001$ compared to the unstimulated control cells $^{*}p < .05$, $^{**}p < .01$ and $^{***}p < .001$ compared to the LPS-treated cells.

3.5. MCD suppressed the LPS-induced JNK/MAPK pathway and phosphorylation of p-c-Jun in macrophages

Based on the significance of the MAPK signaling cascade on the expression of inflammatory mediators and cytokines in macrophages, we examined the effect of MCD on phosphorylation of MAPKs. Phosphorylated JNK, p38 and ERK were enhanced by LPS treatment for 30 min. Interestingly, MCD reduced the phosphorylated JNK level but failed to attenuate phosphorylation of ERK and p38 MAPKs (Fig. 6A and

B). Furthermore, the phosphorylation of c-Jun, a major downstream transcription factor of JNK, was inhibited by MCD in a concentration-dependent manner.

3.6. Effect of MCD on phosphorylation of STAT-1

Activation of TLR4 triggers the phosphorylation of signal transducer and activator of transcription-1 (STAT-1) which also regulates LPS-induced inflammatory response (Shuai and Liu, 2003; Luu et al., 2014).
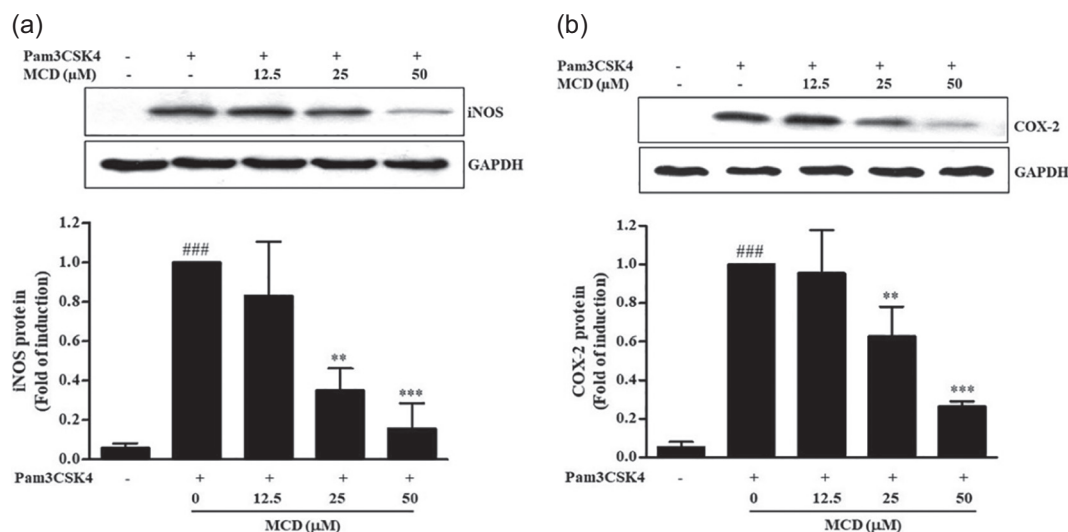
Fig. 4. Inhibition of iNOS and COX-2 expression in Pam3CSK4-stimulated RAW 264.7 macrophages. Cells were treated with MCD in the presence of 1 μg/mL Pam3CSK4 for 24 h. The protein level of iNOS (A) and COX-2 (B) were determined by Western blot analysis. Each column illustrates the mean ± SD of three independent experiments. Data are presented as fold changes of LPS-treated cells. $^{###}p < .001$ compared to unstimulated control cells. $^{**}p < .01$ and $^{***}p < .01$ compared to the LPS-treated cells.

Thus, the effect of MCD on TLR-induced phosphorylation of STAT-1 was determined by Western blot analysis. LPS treatment at 30 min and 60 min led to significant phosphorylation of Ser-727 on STAT-1 while MCD (12.5–50 μM) did not suppress the phosphorylated STAT-1 levels at those time points (Fig. 7A and B).

3.7. Anti-inflammatory effect of MCD in animal models

3.7.1. Effects of MCD on EPP-induced rat ear edema

An EPP-induced ear edema model was carried out as a screening test for determining the anti-inflammatory effect of MCD. After EPP application to the rat ears, the control group demonstrated the greatest degree of ear edema. MCD (3 mg/ear) and the reference drug (phenylbutazone 1 mg/ear) reduced the ear edema at all assessment times. At 1 h after EPP application, the percentage of edema inhibition of MCD and phenylbutazone were 51.5 and 68.9, respectively (data not shown).

3.7.2. Effects of MCD on carrageenan-induced rat paw edema

As shown in Fig. 8, MCD caused a dose-dependent inhibition of paw edema at 1 h, 3 h and 5 h after carrageenan injection. At 3 h, MCD and aspirin at the doses of 300 mg/kg showed significant inhibition to the extents of 45.1% and 70.5%, respectively.

4. Discussion

MCD is a phenolic compound isolated from *E. pavieana* rhizomes with anti-inflammatory properties (Tachai and Nuntawong, 2016; Srisook, Palachot, Mankhong, and Srisook, 2017). Our study demonstrated that MCD has an inhibitory effect on the production of NO and PGE$_2$ in addition to suppressing activation of NF-κB and phosphorylation of JNK and c-Jun. This compound also suppresses inflammatory responses in in vivo rat models.

With LPS stimulation, macrophages secrete a variety of inflammatory mediators and cytokines such as NO and PGE$_2$ (Udomphong, Mankhong, Jaratjaroonphong, and Srisook, 2017; Park et al., 2017). Herein, MCD at the concentrations up to 50 μM exhibited an anti-inflammatory effect without cytotoxicity suggesting that the decrease in the secretion of NO and PGE$_2$ was due to the effect of MCD and not the cell death. This prompted us to investigate the molecular mechanisms underlying its anti-inflammatory property in a LPS-induced macrophage model. The regulation of iNOS-catalyzed NO and

COX-2-catalyzed PGE$_2$ productions is mainly at the transcriptional level (Alderton, Cooper, and Knowles, 2001; Kalinski, 2012). MCD significantly attenuated the protein expressions of iNOS and COX-2 in a concentration-dependent manner. Consistent with the protein suppression, MCD suppressed iNOS and COX-2 mRNA expressions. Thus, MCD possibly inhibited NO and PGE$_2$ productions at both transcriptional and translational levels.

Recently, the TLR2 ligand triacylated lipoprotein Pam3CSK4 was shown to activate iNOS and COX-2 expressions (Shibata et al., 2014; Sang et al., 2018). Similarly, our data showed that activation of either TLR4 by LPS or TLR2/1 by Pam3CSK4 resulted in the expression of iNOS and COX-2 whereas MCD decreased such expressions. It is noted that MCD interfered with not only TLR4 but also the TLR2/1 signal transduction pathway. Furthermore, there have been reports on activation of TLR4 and TLR2/1 triggering the NF-κB signaling downstream effect, such as iNOS and COX-2 expressions (Prekumar, Dey, Dorn, and Raskin, 2010; Shibata et al., 2014; Sang et al., 2018). In unstimulated cells, NF-κB (heterodimers of p65 (relA) and p50) is bound by IκB and retained in the cytoplasm. After activation by various stimuli, including LPS, the NF-κB signaling cascade is triggered, resulting in phosphorylation of IκB by IKK. The phosphorylated IκB is ubiquitylated and degraded, thereby liberating NF-κB. Activated NF-κB moves to the nucleus to modulate the expression of target genes (Won, Byun, Park, and Hur, 2016). In the present study, MCD had a weak inhibitory effect on phosphorylation of IκBα at Ser32/36 and translocation of p65 subunit into the nucleus. The effect of MCD on NF-κB p65 nuclear translocation is consistent with the previous report of 4-methoxycinnamyl *p*-coumarate (MCC), another compound isolated from *E. pavieana* (Mankhong, Iawsipo, Srisook, and Srisook, 2019). These results indicate the suppression of LPS-induced expressions of NO and PGE$_2$ is mediated in part by inactivation of NF-κB pathway via inhibition of IκBα phosphorylation and nuclear translocation of NF-κB p65. Further studies to elucidate the effect of MCD on NF-κB cascade will provide a better understanding of the anti-inflammatory effects of the compound in RAW 264.7 cells.

In addition to the NF-κB pathway, the MAPK cascade participates in LPS-induced expression of inflammatory mediators, (Prekumar, Dey, Dorn, and Raskin, 2010, Baker, Hayden, and Ghosh, 2011, Santos et al., 2011). One downstream cascade triggered by the LPS-TLR4 complex is the MAPK pathway activated by TAK-1 (Achek, Yesudhas, and Choi, 2016). In our study, MCD suppressed the phosphorylation of JNK but
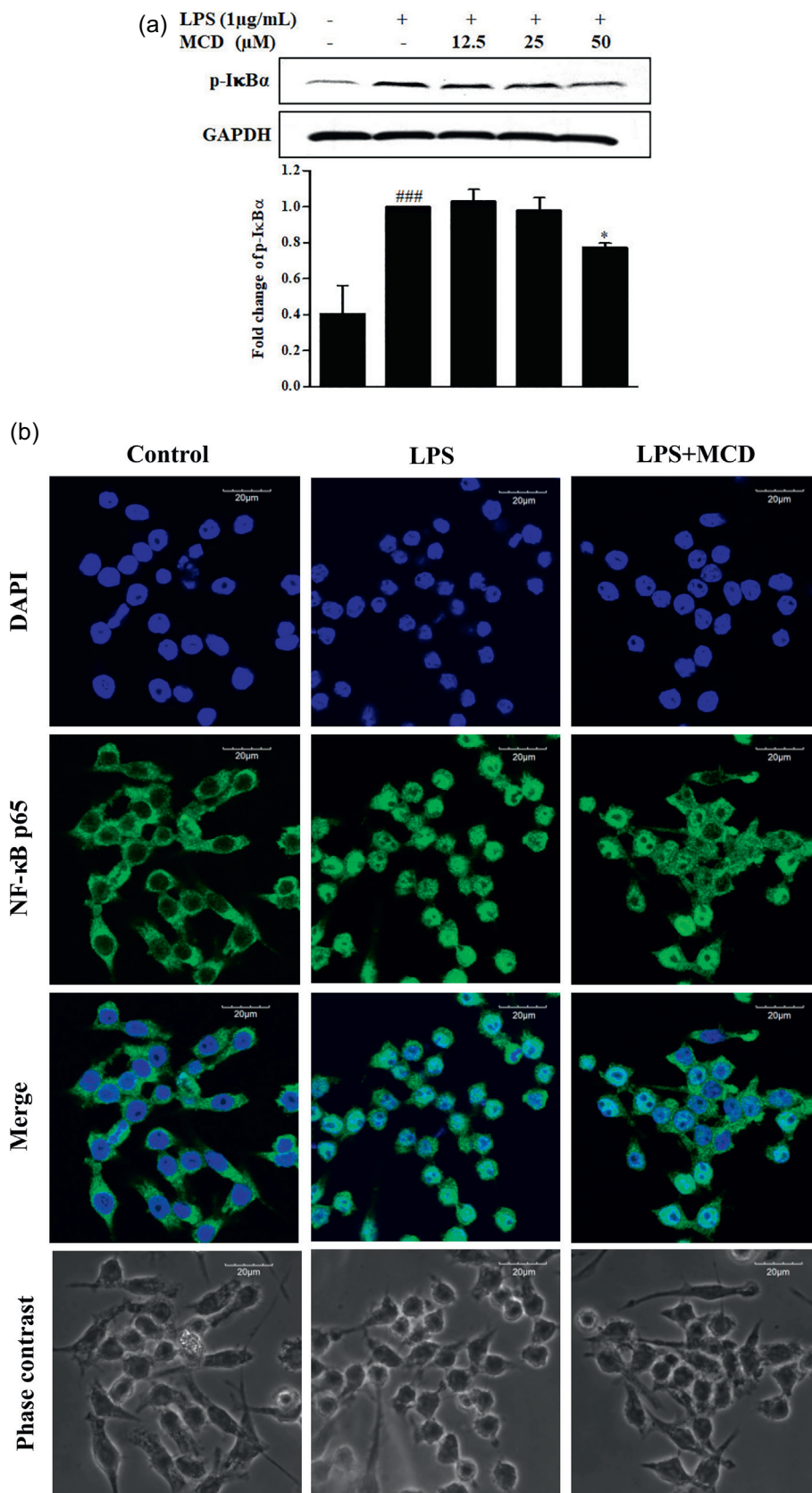
Fig. 5. Effect of MCD on NF-κB activation in LPS-stimulated macrophages. Cells were pretreated with 50 μM of MCD for 1 h, followed by incubation with 1 μg/mL LPS for 30 min. The levels of p-IκB were analyzed by Western blot analysis (A). The graph shows the mean ± SD of results of densitometric analyses of p-IκB, which were normalized to GAPDH densitometric values. (B) Localization of the NF-κB p65 subunit was investigated by immunofluorescence under a confocal laser scanning microscope. Nuclei were counterstained with DAPI. $^{###}p < .001$ compared to the unstimulated control cells. $^{*}p < .05$ compared to the LPS-treated cells.
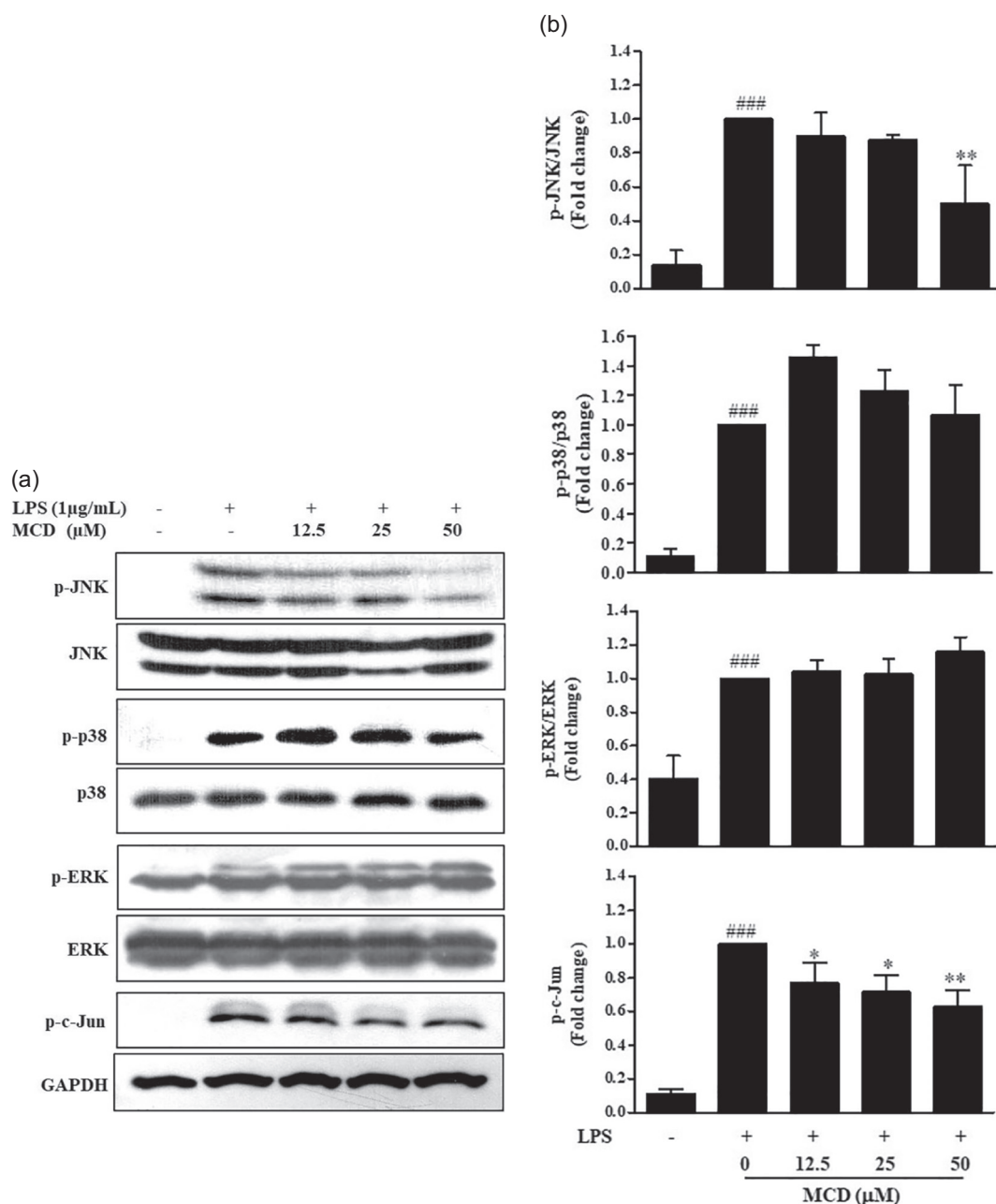
Fig. 6. Effect of MCD on LPS-induced phosphorylation of MAPKs in macrophages. Cells were incubated with 12.5–50 μM of MCD before treating with 1 μg/mL LPS for 30 min. The phosphorylated and total form of MAPKs were detected by Western blot analysis. The graph shows the mean ± SD from densitometric analyses of phosphorylation levels of JNK, p38 MAPK and ERK1/2, which were normalized to the total levels of JNK, p38 MAPK and ERK1/2 densitometric values, respectively. Data are presented as fold changes of LPS-treated cells. $^{##}p < .01$ and $^{###}p < .001$ compared to the unstimulated control cells. $^{**}p < .01$ compared to the LPS-treated cells.

did not cause a decrease in the level of LPS-induced ERK and p38 MAPK phosphorylation. The major downstream transcription factor activated by JNK is AP-1, which usually forms heterodimers or homodimers consisting of Jun, Fos and ATF proteins (Liew et al., 2011; Hannemann et al., 2017). AP-1 activation is mediated, in part, by JNK-stimulated phosphorylation of c-Jun, its major component (Raivich et al., 2004). MCD attenuated LPS-induced c-Jun phosphorylation indicating inhibition of the AP-1 activity. Thus, our data suggested that, apart from the NF-κB pathway, MCD might exert its anti-inflammatory property by preventing JNK activation, which in turn inhibits phosphorylation of c-Jun. Although the present study does not clarify how MCD inhibits JNK activation, the results suggest that MCD inhibits the inflammatory response possibly through the suppression of upstream signaling of the

JNK cascade. In accordance with our results, hispidulin (Srisook et al., 2015) and 2′-benzoyloxycinnamaldehyde's anti-inflammatory properties have been attributed to the impediment of NF-κB activation and JNK phosphorylation in the RAW 264.7 cell model (Kwon et al., 2011). To the contrary, our recent study reported that the anti-inflammatory activity of MCC from *E. pavieana* was mediated via inactivation of the Akt/c-Jun signaling pathways but was independent of MAPKs pathways (Mankhong, Iawsipo, Srisook, and Srisook, 2019). The different effect of MCD and MCC on MAPK signaling might result from the structural differences.

STAT-1 pathway has also been shown to regulate the expression of inflammatory responsive genes including iNOS and COX-2 (Liew et al., 2011; Han, Shin, Lee, Park, and Lee, 2018) and LPS triggers TLR4
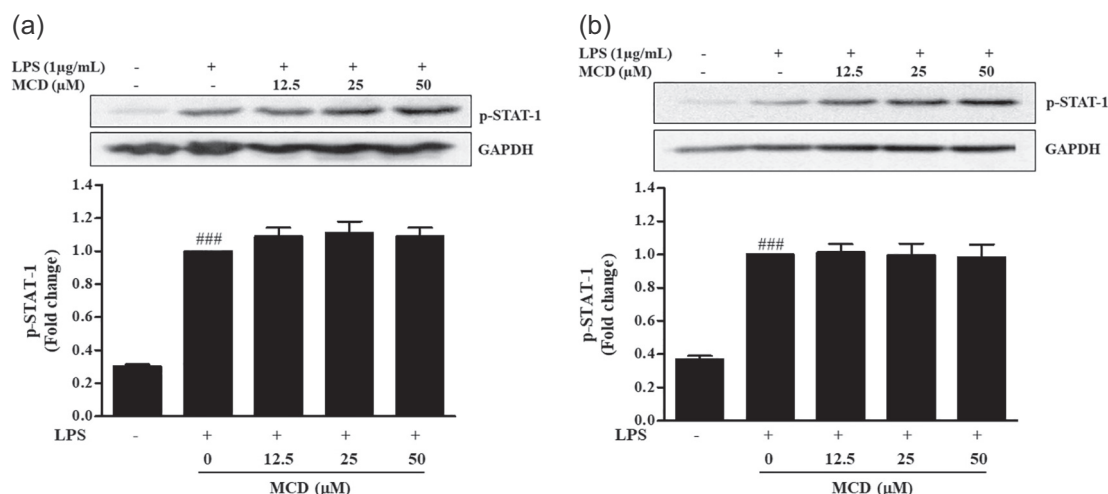
Fig. 7. Effect of MCD on LPS-induced STAT-1 Ser-727 phosphorylation. Cells were incubated with MCD for 1 h prior to treating with 1 μg/mL LPS for 30 (A) and 60 (B) min. The phosphorylated STAT-1 was detected by Western blot analysis. The graph shows the mean ± SD from densitometric analyses of phosphorylation levels of STAT-1, which were normalized to the total protein of GAPDH. Data are presented as fold changes of LPS-treated cells. $^{###}p < .001$ compared to the unstimulated control cells.
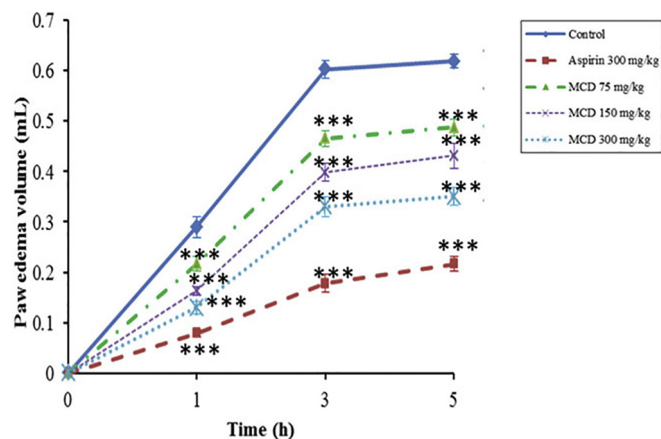
Fig. 8. The effects of administration of MCD (75, 150 and 300 mg/kg, p.o.) or aspirin (300 mg/kg, p.o.) on rat paw edema induced by carrageenan injection. Treatment effects were analyzed using an ANOVA and post hoc least-significant difference (LSD) test. $^{***}p < .001$ compared to the control group.

signaling cascade leading to phosphorylation of STAT-1 at Ser-727 (Rhee, Jones, Toshchakov, Vogel, and Fenton, 2003). We therefore investigated whether MCD inhibits inflammatory response via the STAT-1 pathway. From this study, it is likely that MCD failed to abolish the phosphorylated STAT-1 (Ser-727) levels in LPS-induced RAW 264.7 macrophages. These results suggest that anti-inflammatory effect of MCD in macrophages is not mediated by the STAT-1 pathway.

The in vivo anti-inflammatory effect of MCD was evaluated using EPP-induced ear edema and carrageenan-induced paw edema models. EPP-induced rat ear edema is the well-known screening test for the anti-inflammatory effect of chemicals or natural products (Eddouks, Chattopadhyay, and Zeggwagh, 2012). Edema formation induced by EPP is attributed to a release of several inflammatory mediators (Carlson, O'Neill-Davis, Chang, and Lewis, 1985). The second animal model used in this study was carrageenan-induced paw edema. It is believed to be three distinct phases of mediator release. The first phase begins immediately after injection of carrageenan, which is mediated by histamine and serotonin. The second phase is associated with the release of bradykinin, and the third phase is attributed to the synthesis and release of several inflammatory mediators, especially prostaglandins and NO (Liao et al., 2012; Mansouri et al., 2015). In the

carrageenan-induced edema model, the inflammatory response is usually determined by an increase in paw volume. It was found that the pretreatment of MCD to the rats in the test groups significantly inhibited the inflammatory response caused by EPP and carrageenan. These results revealed the in vivo anti-inflammatory effect of MCD. As MCD markedly suppressed the production of NO and PGE_2 in LPS-induced RAW 264.7 macrophages, this implied the mode of MCD anti-inflammatory action in the carrageenan-induced edema model might be in part due to the inhibition of the NO and PGE_2 productions as well.

In conclusion, our results suggest that MCD's inhibitory effect on an immune response acts in macrophages by blocking NF-κB and JNK/c-Jun signaling pathways but not STAT-1, leading to the suppression of iNOS and COX-2 expressions and ultimately their productions. MCD also inhibited inflammatory responses in a rat model. Our data, therefore, demonstrate the potential of using MCD in the development of a novel anti-inflammatory agent from natural products for the treatment of inflammation-related diseases.

Conflict of interests

The authors have no conflict of interest to declare.

Acknowledgements

References

Abbas, A.K., Lichtman, A.H., 2003. Cellular and Molecular Immunology, 5th ed. Saunders, Philadelphia.
Achek, A., Yesudhas, D., Choi, S., 2016. Toll-like receptors: promising therapeutic targets for inflammatory diseases. Arch. Pharm. Res. 39, 1032–1049.
Alderton, K.W., Cooper, E.C., Knowles, G.R., 2001. Nitric oxide synthases: structure, function and inhibition. Biochem. J. 357, 593–615.
Baker, R.G., Hayden, M.S., Ghosh, S., 2011. NF-κB, inflammation and metabolic disease. Cell Metab. 13, 11–22.
Brattsand, R., Thalen, A., Roempke, K., Kallstrom, L., Gruvstad, E., 1982. Influence of 16 alpha, 17 alpha-acetal substitution and steroid nucleus fluorination on the topical to systemic activity ratio of glucocorticoids. J. Steroid Biochem. Mol. Biol. 16, 779–786.

Carlson, R., O'Neill-Davis, L., Chang, J., Lewis, A., 1985. Modulation of mouse ear edema by cyclooxygenase and lipoxygenase inhibitors and other pharmacologic agents. Agents Actions 17, 197–204.

Christiansen, O.B., Nielsen, H.S., Kolte, A.M., 2006. Inflammation and miscarriage. Semin. Fetal Neonatal Med. 11, 302–308.

Eddouks, M., Chattopadhyay, D., Zeggwagh, N.A., 2012. Animal models as tools to investigate antidiabetic and anti-inflammatory plants. Evid. Based Complement. Alternat. Med. 2012https://doi.org/10.1155/2012/142087. Article ID 142087.

Fujiwara, N., Kobayashi, K., 2005. Macrophages in inflammation. Current Drug Targets - Inflamm. Aller. 4, 281–286.

Giulietti, A., Overbergh, L., Valckx, D., Decallonne, B., Bouillon, R., Mathieu, C., 2001. An overview of real-time quantitative PCR: applications to quantify cytokine gene expression. Methods 25, 386–401.

Han, H.S., Shin, J.S., Lee, S.B., Park, J.C., Lee, K.T., 2018. Cirsimarin, a flavone glucoside from the aerial part of *Cirsium japonicum var. ussuriense* (Regel) Kitam. ex Ohwi, suppresses the JAK/STAT and IRF-3 signaling pathway in LPS-stimulated RAW 264.7 macrophages. Chem. Biol. Interact. 293, 38–47.

Hannemann, N., Jordan, J., Paul, S., Reid, S., Baenkler, H.W., Sonnewald, S., Bäuerle, T., Vera, J., Schett, G., Bozec, A., 2017. The AP-1 transcription factor c-Jun promotes arthritis by regulating cyclooxygenase-2 and arginase-1 expression in macrophages. J. Immunol. 198, 3605–3614.

Iawsipo, P., Srisook, E., Ponglikitmongkol, M., Tatiyar, S., Singaed, O., 2018. Cytotoxic effects of *Etlingera pavieana* rhizome on various cancer cells and identification of a potential anti-tumor component. J. Food Biochem. 1–9 e12540.

Kalinski, P., 2012. Regulation of immune responses by prostaglandin E$_2$. J. Immunol. 188, 21–28.

Kwon, J.Y., Hong, S.H., Park, S.D., Ahn, S.G., Yoon, J.H., Kwon, B.M., Kim, S.A., 2011. 2′-Benzoyloxycinnamaldehyde inhibits nitric oxide production in lipopolysaccharide-stimuated RAW 264.7 cells via regulation of AP-1 pathway. Eur. J. Pharmacol. 696, 179–186.

Liao, J.C., Deng, J.S., Chiu, C.S., Hou, W.C., Huang, S.S., Shie, P.S., Huang, G.J., 2012. Anti-inflammatory activities of *Cinnamomum cassia* constituents in vitro and in vivo. Evid. Based Complement. Alternat. Med. 2012https://doi.org/10.1155/2012/429320. Article ID 429320.

Liew, C.Y., Lam, K.W., Kim, M.K., Harith, H.H., Tham, C.L., Cheah, Y.K., Sulaiman, M.R., Lajis, N.H., Israf, D.A., 2011. Effects of 3-(2-Hydroxyphenyl)-1-(5-methyl-furan-2-y-l) propenone (HMP) upon signaling pathways of lipopolysaccharide-induced iNOS synthesis in RAW 264.7 cells. Int. Immunopharmacol. 11, 85–95.

Lu, Y.C., Yeh, W.C., Ohashi, S.P., 2008. LPS/TLR4 signal transduction pathway. Cytokine 42, 145–151.

Luu, K., Greenhill, C.J., Majoros, A., Decker, T., Jenkins, B.J., Mansell, A., 2014. STAT1 plays a role in TLR signal transduction and inflammatory responses. Immunol. Cell Biol. 92, 761–769.

Mankhong, S., Iawsipo, P., Srisook, E., Srisook, K., 2019. 4-methoxycinnamyl *p*-coumarate isolated from *Etlingera pavieana* rhizomes inhibits inflammatory response via suppression of NF-κB, Akt and AP-1 signaling in LPS-stimulated RAW 264.7 macrophages. Phytomedicine 54, 89–97.

Mansouri, M.T., Hemmati, A.A., Naghizadeh, B., Mard, S.A., Rezaie, A., Ghorbanzadeh, B., 2015. A study of the mechanisms underlying the anti-inflammatory effect of ellagic acid in carrageenan-induced paw edema in rats. Indian J. Pharm. 47, 292–298.

Park, J.Y., Chung, T.W., Jeong, Y.J., Kwak, C.H., Ha, S.H., Kwan, K.M., Abekura, F., Cho, S.H., Lee, Y.C., Ha, K.T., Magae, J., Chang, Y.C., Kim, C.H., 2017. Ascofuranone inhibits lipopolysaccharide-induced inflammatory response via NF- kappaB and AP-1, p-ERK, TNF-α, IL-6 and IL-1β in RAW 264.7 macrophages. PLoS One 12, 1–14.

Poulsen, D.A., Phonsena, P., 2017. Morphological variation and distribution of the useful ginger *Etlingera pavieana* (Zingiberaceae). Nord. J. Bot. 35, 467–475.

Prekumar, V., Dey, M., Dorn, R., Raskin, I., 2010. MyD88-dependent and independent pathways of toll-like receptors are engaged in biological activity of Triptolide in ligand-stimulated macrophages. BMC Chem. Biol. 10, 1–13.

Qureshi, A.A., Tan, X., Reis, J.C., Badr, M.Z., Papasian, C.J., Morrison, D.C., Qureshi, N., 2011. Suppression of nitric oxide induction and pro-inflammatory cytokines by novel proteasome inhibitors in various experimental models. Lipids Health Dis. https://doi.org/10.1186/1476-511X-10-177. 1-25.

Raivich, G., Bohatschek, M., Da Costa, C., Aguzzi, A., Wagner, E.F., Behrens, A., 2004. The AP-1 transcription factor c-Jun is required for efficient axonal regeneration. Neuron 43, 57–67.

Rhee, S.H., Jones, B.W., Toshchakov, V., Vogel, S.N., Fenton, M.J., 2003. Toll-like receptors 2 and 4 activate STAT1 serine phosphorylation by distinct mechanisms in macrophages. J. Biol. Chem. 278, 22506–22512.

Sang, W., Zhong, Z., Linghu, K., Xiong, W., Tse, A.K.W., Cheang, W.S., Yu, H., Wang, Y., 2018. *Siegesbeckia pubescens* Makino inhibits Pam3CSK4-induced inflammation in RAW 264.7 macrophages through suppressing TLR1/ TLR2-mediated NF-κB activation. Chin. Med. 13, 37. https://doi.org/10.1186/s13020-018-0193-x.

Santos, R.C.V., Rico, M.A.P., Bartrons, R., Pujol, F.V., Rosa, J.L., de Oliveira, J.R., 2011. The transcriptional activation of the cyclooxygenase-2 gene in zymosan-activated macrophages is dependent on NF-kappa B, C/EBP, AP-1, and CRE sites. Inflammation 34, 653. https://doi.org/10.1007/s10753-010-9275-3.

Sharma, U.K., Sood, S., Sharma, N., Rahi, P., Kumar, R., Sinha, A.K., Gulati, A., 2013. Synthesis and SAR investigation of natural phenylpropene-derived methoxylated cinnamaldehydes and their novel Schiff bases as potent antimicrobial and antioxidant agents. Med. Chem. Res. 22, 5129–5140.

Shibata, T., Nakashima, F., Honda, K., Lu, Y.J., Kondo, T., Ushida, Y., Aizawa, K., Suganuma, H., Oe, S., Tanaka, H., Takahashi, T., Uchida, K., 2014. Toll-like receptors as a target of food-derived anti-inflammatory compounds. J. Biol. Chem. 289, 32757–32772.

Shuai, K., Liu, B., 2003. Regulation of JAK-STAT signalling in the immune system. Nat. Rev. Immunol. 3, 900–911.

Srisook, K., Palachot, M., Mongkol, N., Srisook, E., Sarapusit, S., 2011. Anti-inflammatory effect of ethyl acetate extract from *Cissus quadrangularis* Linn may be involved with induction of heme oxygenase-1 and suppression of NF-kappaB activation. J. Ethnopharmacol. 133, 1008–1014.

Srisook, K., Srisook, E., Nachaiyo, W., Chan-In, M., Thongbai, J., Wongyoo, K., Chawsuanthong, S., Wannasri, K., Intasuwan, S., Watcharanawee, K., 2015. Bioassay-guided fractionation of anti- inflammatory agents from *Clerodendrum inerme* (L.) Gaertn. Leaves and its mechanistic action through the suppression of iNOS and COX-2 pathways in LPS-induced RAW 264.7 macrophages. J. Ethnopharmacol. 165, 94–102.

Srisook, E., Palachot, M., Mankhong, S., Srisook, K., 2017. Anti-inflammatory effect of *Etlingera pavieana* (Pierre ex Gagnep.) R.M.Sm. rhizomal extract and its phenolic compound in lipopolysaccharide-stimulated macrophages. Pharmacogn. Mag. 13, S230–S235.

Tachai, S., Nuntawong, N., 2016. Uncommon secondary metabolites from *Etlingera pavieana* rhizomes. Nat. Prod. Res. 30, 2215–2219.

Udomphong, S., Mankhong, S., Jaratjaroonphong, J., Srisook, K., 2017. Involvement of p38 MAPK and ATF-2 signaling pathway in anti-inflammatory effect of a novel compound bis [(5-methyl)2-furyl] (4- nitrophenyl) methane on lipopolysaccharide-stimulated macrophages. Int. Immunopharmacol. 50, 6–13.

Wang, K.C., Chang, J.S., Chiang, L.C., Lin, C.C., 2009. 4-Methoxycinnamaldehyde inhibited human respiratory syncytial virus in a human larynx carcinoma cell line. Phytomedicine 16, 882–886.

Winter, C.A., Risley, E.A., Nuss, G.W., 1962. Carrageenin-induced edema in hind paw of the rat as an assay for anti-inflammatory drugs. In: Proceedings of the Society for Experimental Biology and Medicine. vol. 11. pp. 544–547.

Won, M., Byun, H.S., Park, K.A., Hur, G.M., 2016. Post-translational control of NF-κB signaling by ubiquitination. Arch. Pharm. Res. 39, 1075–1084.